Variance-reduced estimator of the connected two-point function in the presence of a broken $\mathbb{Z}_2$-symmetry

Martin Hasenbusch*
Institut für Physik, Humboldt-Universität zu Berlin, Newtonstrasse 15, 12489 Berlin, Germany
(Received 15 December 2015; published 23 March 2016)

The exchange or geometric cluster algorithm allows us to define a variance-reduced estimator of the connected two-point function in the presence of a broken $\mathbb{Z}_2$-symmetry. We present numerical tests for the improved Blume-Capel model on the simple-cubic lattice. We perform simulations for the critical isotherm, the low-temperature phase at vanishing external field, and, for comparison, also the high-temperature phase. For the connected two-point function, a substantial reduction of the variance can be obtained, allowing us to compute the correlation length ξ with high precision. Based on these results, estimates for various universal amplitude ratios that characterize the universality class of the three-dimensional Ising model are computed.

DOI: 10.1103/PhysRevE.93.032140

I. INTRODUCTION

Cluster algorithms [1,2] have drastically reduced autocorrelation times in Monte Carlo simulations of a certain class of spin models. In particular for the Ising model, critical slowing down could be virtually eliminated. In addition, cluster algorithms allow us to introduce variance-reduced estimators of the two-point function. In the case of the Swendsen-Wang algorithm, after freezing or deleting links, the remaining degrees of freedom are the overall signs of the clusters. The variance-reduced or improved estimator is constructed by performing the sum over these degrees of freedom exactly [3–5]. This allowed the magnetic susceptibility and the correlation length of the Ising model and also $O(N)$-invariant nonlinear σ-models with $N > 1$ in the disordered phase to be determined to high precision. See for example Refs. [6,7]. However, in the presence of a broken symmetry, these estimators fail to reduce the variance significantly.

The exchange cluster algorithm [8,9] is closely related with the geometric cluster algorithm [10]. In the exchange cluster algorithm, a pair of systems is considered. These systems do not interact. Hence the Hamiltonian of the pair is just given by the sum of the two Hamiltonians. In the exchange cluster algorithm, the values of spins at corresponding sites are exchanged between the two systems. Since the total sum of the spins stays constant under such updates, the exchange cluster algorithm is not ergodic. Therefore, in addition, updates of the individual systems with, for example, the local heat-bath and standard cluster algorithms are performed. In the geometric cluster algorithm, only a single system is considered. The sites of the lattice are grouped into pairs. The values of the spins are exchanged within these pairs. The authors of [8,9] were mainly aiming at systems with external fields. Here the virtue of the algorithm is that the external field does not effect the exchange of the spins. Therefore, particularly in the case of the Ising model in a random field, one would expect a reduction of autocorrelation times [11].

In [12,13], we used the exchange cluster algorithm to get variance-reduced estimators of quantities related to the thermodynamic Casimir force. Here, we discuss a variance-reduced estimator of the connected two-point correlation function in the presence of a broken $\mathbb{Z}_2$-symmetry. We study the properties of this estimator in the example of the Blume-Capel model on the simple-cubic lattice. Its reduced Hamiltonian is given by

$$H = -\beta \sum_{\langle xy \rangle} s_x s_y + D \sum_x s_x^2 - h \sum_x s_x, \tag{1}$$

where the spin might assume the values $s_x \in \{-1,0,1\}$. $x = (x_0,x_1,x_2)$ denotes a site on the simple-cubic lattice, where $x_i \in \{1,2,\ldots,L_i\}$, and $\langle xy \rangle$ denotes a pair of nearest neighbors on the lattice. We impose periodic boundary conditions in all three directions. In our numerical study, we consider lattices with the same linear extension $L = L_0 = L_1 = L_2$ in all directions. The inverse temperature is given by $\beta = 1/k_B T$, D controls the density of vacancies $s_x = 0$, and h is an external field. One finds that for $D^* = 0.656(20)$, leading corrections to scaling vanish [14]. Here we shall study the model at $D = 0.655$, where $\beta_c = 0.387\,721\,735(25)$ is known with high precision [14].

The paper is organized as follows. First we recall the definition of the exchange cluster algorithm and discuss the construction of the variance-reduced estimator of the connected two-point function. Next we discuss the definition of the second-moment and the exponential correlation length. We recall how these quantities are determined from the connected two-point function that we compute in the Monte Carlo simulation. Theoretical predictions for the behavior of the slice-slice correlation function are summarized. Then we summarize some results for critical phenomena that are needed for the analysis of our data. Following that, there is a discussion of our numerical study. We briefly discuss the update scheme that is used. The behavior of the statistical error of the slice-slice correlation function is analyzed. Based on our data, we study the critical behavior in the high- and low-temperature phase and on the critical isotherm. Here we are mainly aiming at universal amplitude ratios. We summarize our results and give an outlook. In the Appendix, we briefly summarize results that we obtained for the critical isotherm of the standard Ising model.

*martin.hasenbusch@physik.hu-berlin.de

II. THE CONNECTED TWO-POINT FUNCTION: VARIANCE REDUCTION

Let us start the discussion assuming $h > 0$, such that the $\mathbb{Z}_2$-symmetry is explicitly broken. The connected two-point function is defined by $G(x-y) = \langle s_x s_y\rangle - \langle s_x\rangle\langle s_y\rangle$, where $\langle s_x\rangle = \langle s_y\rangle = m$ is the magnetization of the system. Now let us consider a pair of identical systems. The two-point function of the difference of the spins in these two systems is

$$\begin{aligned} G_2(x-y) &= \langle (s_{x,1}-s_{x,2})(s_{y,1}-s_{y,2})\rangle \\ &= \langle s_{x,1}s_{y,1}\rangle + \langle s_{x,2}s_{y,2}\rangle - \langle s_{x,2}s_{y,1}\rangle - \langle s_{x,1}s_{y,2}\rangle, \end{aligned} \tag{2}$$

where the second index of $s_{x,l}$ with $l \in \{1,2\}$ denotes the system. Since the two systems do not interact, $\langle s_{x,2}s_{y,1}\rangle = \langle s_{x,2}\rangle\langle s_{y,1}\rangle = m^2$ and hence $G_2(x-y) = 2G(x-y)$.

Now let us apply the exchange cluster algorithm to the pair of systems. The elementary operation of the algorithm is to swap the value of spins between the two systems. This can be written in terms of an auxiliary Ising variable $\sigma_x \in \{-1,1\}$:

$$\begin{aligned} \tilde{s}_{x,1} &= \frac{1+\sigma_x}{2}s_{x,1} + \frac{1-\sigma_x}{2}s_{x,2}, \\ \tilde{s}_{x,2} &= \frac{1-\sigma_x}{2}s_{x,1} + \frac{1+\sigma_x}{2}s_{x,2}. \end{aligned} \tag{3}$$

For $\sigma_x = -1$, the exchange is performed, while for $\sigma_x = 1$ the old values are kept. Now we update the σ_x using the Swendsen-Wang cluster algorithm. The construction of the clusters is characterized by the probability to delete the link $\langle xy\rangle$ between the nearest neighbors x and y [10]:

$$p_d = \min[1, \exp(-2\beta_{\text{embed}})], \tag{4}$$

where $\beta_{\text{embed}} = \frac{\beta}{2}(s_{x,1}-s_{x,2})(s_{y,1}-s_{y,2})$. A link $\langle xy\rangle$ that is not deleted is called frozen. As for the cluster algorithm [1,2] applied to the Ising model, clusters are sets of sites that are connected by frozen links. For all sites x within a given cluster $\sigma_x = \hat{\sigma}_i$, where i labels the clusters. Hence the remaining degrees of freedom are the $\hat{\sigma}_i = \pm 1$, with equal weight for each of the two possible values. Variance-reduced estimators are obtained by performing the average over all possible configurations of the $\hat{\sigma}_i$ exactly. For the estimator $A_2 = (s_{x,1}-s_{x,2})(s_{y,1}-s_{y,2})$ we get the variance-reduced counterpart

$$\begin{aligned} A_{2,\text{imp}} &= \frac{1}{2^{N_c}}\sum_{\hat{\sigma}}[\sigma_x(s_{x,1}-s_{x,2})][\sigma_y(s_{y,1}-s_{y,2})] \\ &= \frac{1}{2^{N_c}}\sum_{\hat{\sigma}}\hat{\sigma}_{i|x\in i}\hat{\sigma}_{j|y\in j}(s_{x,1}-s_{x,2})(s_{y,1}-s_{y,2}) \\ &= \Theta(x,y)\,(s_{x,1}-s_{x,2})(s_{y,1}-s_{y,2}), \end{aligned} \tag{5}$$

where N_c is the number of clusters and $\Theta(x,y)$ is equal to 1 if x and y belong to the same cluster and 0 otherwise. Inspecting Eq. (4), we see that $p_d < 1$ requires that $(s_{x,1}-s_{x,2})(s_{y,1}-s_{y,2}) > 0$. Hence the difference $(s_{x,1}-s_{x,2})$ has the same sign for all sites x in a given cluster. Hence $A_{2,\text{imp}} \geqslant 0$, which is obviously not the case for the standard estimator A_2.

Next let us discuss the case of spontaneous symmetry breaking in the low-temperature phase. The problem is that for $h = 0$ there is no symmetry breaking on a finite lattice. In analytical calculations, one therefore introduces a finite external field h and takes the thermodynamic limit at finite h first and then performs the limit $h \searrow 0$. In Monte Carlo simulations, it is too cumbersome to mimic this approach. Therefore, usually the magnetization at $h = 0$ is computed as

$$m = \frac{1}{L_0L_1L_2}\left\langle\left|\sum_x s_x\right|\right\rangle. \tag{6}$$

This is motivated by the hypothesis that the partition function is dominated by configurations that can be clearly assigned to one of the bulk phases, while the remainder is again dominated by configurations in which two interfaces separate regions that can be assigned to the bulk phases. The contribution of the latter configurations is, at least in the most simple approximation, proportional to $\exp(-2\sigma L^2)$, where σ is the interface tension. For a more detailed discussion, see the vast literature on the physics of interfaces. See, for example, Ref. [15] and references therein.

In the same spirit, we align the magnetization of the two systems here. To simplify the discussion, we ignore configurations with exactly vanishing magnetization in the following. First note that the constraint $M_1M_2 > 0$, where $M_l = \sum_x s_{x,l}$ does not affect the marginal distributions of the individual systems $l = 1$ and 2. Concerning the estimator of the two-point function, the discussion below Eq. (2) has to be slightly modified:

$$\begin{aligned} \langle s_{x,2}s_{y,1}\rangle &= \langle s_{x,1}s_{y,2}\rangle \\ &= \left\langle \frac{1}{L_0L_1L_2}\sum_u s_{u,1}\ \ \frac{1}{L_0L_1L_2}\sum_w s_{w,2}\right\rangle \\ &= \left\langle \frac{1}{L_0L_1L_2}\left|\sum_u s_{u,1}\right|\ \ \frac{1}{L_0L_1L_2}\left|\sum_w s_{w,2}\right|\right\rangle \\ &= m^2, \end{aligned} \tag{7}$$

where we used that the two systems are uncorrelated up to the constraint $M_1M_2 > 0$.

Now let us discuss how this constraint is imposed in the simulation. Updating the individual systems by using local or cluster algorithms leaves the Boltzmann distributions of the individual systems invariant. However, the resulting configurations might violate the constraint $M_1M_2 > 0$. This could be reinforced by hand: If $M_1M_2 < 0$, we simply multiply all spins in the first system by -1. Since $M_2 > 0$ and $M_2 < 0$ are equally probable, this operation leaves invariant the Boltzmann distribution of the first system. Now the aligned configurations are updated with the exchange cluster algorithm, and the improved estimator (5) is computed. The remaining problem is that the exchange cluster algorithm does not strictly leave the constraint $M_1M_2 > 0$ invariant. By construction $M_1 + M_2$ is kept constant. Based on the hypothesis on the probability distribution of the magnetization discussed above, the probability that M_1M_2 changes sign under the exchange cluster algorithm is at least suppressed by a factor of $\exp(-2\sigma L^2)$.

In our simulations, we actually considered the quantity

$$P = \sum_x s_{x,1}s_{x,2}, \tag{8}$$

which is invariant under the exchange of spins between the configurations. We replaced the constraint $M_1 M_2 > 0$ by $P > 0$. This means that after performing the updates of the individual systems, we determine P, and if $P < 0$ the spins of the first system are multiplied by -1. The remaining question is, how likely is $M_1 M_2 > 0$ given $P > 0$? In fact, our numerical results show that with increasing L, the probability rapidly goes to 1.

III. THE CORRELATION LENGTH AND THE SPECTRUM OF THE TRANSFER MATRIX

In our study, we are aiming at the magnetic susceptibility and the correlation length, which are derived from the two-point function. Here we briefly recall some basic definitions. For a more detailed discussion, see, for example, Sec. 4 of Ref. [16].

To simplify the analysis, one projects to zero-momentum states of the transfer matrix. Toward that end, one considers the correlation function $\bar{G}(r) = \langle S_0 S_r \rangle - \langle S_0 \rangle \langle S_r \rangle$ of slices

$$S_{x_0} = \frac{1}{\sqrt{L_1 L_2}} \sum_{x_1, x_2} s_{(x_0, x_1, x_2)}. \tag{9}$$

For finite L_1, L_2, and $L_0 \to \infty$, assuming $r \geqslant 0$, the slice-slice correlation function has the form

$$\bar{G}(r) = \sum_{\alpha} c_\alpha \exp(-m_\alpha r), \tag{10}$$

where

$$c_\alpha = \langle 0|S|\alpha\rangle^2, \tag{11}$$

where $|\alpha\rangle$ are the eigenvectors of the transfer matrix. $|0\rangle$ is the eigenvector corresponding to the largest eigenvalue λ_0. Since the transfer matrix is a real, symmetric, and positive-definite matrix, the eigenvalues λ_α are real and positive. Let us assume that they are ordered such that $\lambda_\alpha \geqslant \lambda_\beta$ for $\alpha < \beta$. The masses are given by $m_\alpha = -\ln(\lambda_\alpha/\lambda_0)$. In the basis of slice configurations, S is a diagonal matrix with entries given by Eq. (9). The coefficient c_α is nonvanishing only if $|\alpha\rangle$ has zero momentum, zero angular momentum, and positive parity. For a more detailed discussion of the transfer-matrix formalism, see, for example, Sec. 4.1 of Ref. [16]. In the limit $L_1, L_2 \to \infty$, the dimension of the transfer matrix rapidly goes to infinity. One expects that the slice-slice correlation function assumes the form

$$\bar{G}(r) = \sum_i c_i \exp(-m_i r) + \sum_j f_{\mathrm{cut},j}(r). \tag{12}$$

In a particle interpretation, m_1 is the mass of the fundamental particle, while the m_i with $i > 1$ can be interpreted as masses of bound states of the fundamental particle. The contributions

$$f_{\mathrm{cut},j}(r) = \int_{\mu_{0,j}}^{\mu_{\max,j}} d\mu\, a_j(\mu) \exp(-\mu r) \tag{13}$$

are due to scattering states. Therefore, $\mu_{0,j} = \sum_i n_{i,j} m_i$, where $n_{i,j}$ is an integer and $\sum_i n_{i,j} > 1$. For the theoretical background, see textbooks on quantum field theory, such as, for example, [17]. Explicit results for the three-dimensional Ising universality class are summarized below in Sec. III A.

The exponential correlation length is defined by the decay of the correlation function at large distances. Hence $\xi_{\mathrm{exp}} = 1/m_1$. Analyzing data obtained from Monte Carlo simulations, one often considers the effective correlation length

$$\xi_{\mathrm{eff}}(r) = -1/\ln\left[\frac{\bar{G}(r+1/2)}{\bar{G}(r-1/2)}\right]. \tag{14}$$

The exponential correlation length is obtained as $\xi_{\mathrm{exp}} = \lim_{r\to\infty} \xi_{\mathrm{eff}}(r)$.

The second-moment correlation length is defined by $\xi_{\mathrm{2nd}}^2 = \frac{\mu_2}{2d\chi}$, where $d = 3$ in our case and the magnetic susceptibility can be written as $\chi = \bar{G}(0) + 2\sum_{r=1}^{\infty} \bar{G}(r)$ and $\mu_2 = 2d \sum_{r=1}^{\infty} r^2 \bar{G}(r)$. For a single exponential decay, $\bar{G}(r) = c\ \exp(-r/\xi_{\mathrm{exp}})$, one gets

$$\xi_{\mathrm{2nd,single}}^2 = \frac{\exp[-1/\xi_{\mathrm{exp}}]}{(1 - \exp[-1/\xi_{\mathrm{exp}}])^2} \tag{15}$$

for the second-moment correlation length. In the limit $\xi_{\mathrm{exp}} \to \infty$, one gets $\xi_{\mathrm{exp}}/\xi_{\mathrm{2nd,single}} = 1 + O(1/\xi_{\mathrm{exp}}^2)$. For example, for $\xi_{\mathrm{exp}} = 1$, we get $\xi_{\mathrm{exp}}/\xi_{\mathrm{2nd,single}} = 1.042\,19\ldots$.

In fact, $\bar{G}(r)$ is dominated by a single exponential decay. Therefore, we have multiplied $\xi_{\mathrm{exp}}/\xi_{\mathrm{2nd}}$ by

$$z_{\mathrm{cor}} = \xi_{\mathrm{2nd,single}}/\xi_{\mathrm{exp}} \tag{16}$$

in our numerical analysis to reduce finite ξ_{exp} corrections. Analyzing our Monte Carlo data, we computed χ and μ_2 in the following way: Up to a certain distance R, we have used $\bar{G}(r)$ computed directly from the configurations that we have generated. Since the relative statistical error increases exponentially with the distance r, for $r > R$ we have used instead

$$\tilde{G}(r) = \bar{G}(R) \exp\left(-\frac{r-R}{\xi_{\mathrm{eff}}(R+1/2)}\right). \tag{17}$$

We will comment on the choice of R below. Also note that, in order to reduce the statistical error, we computed the slice-slice correlation function for all three directions of the lattice. Furthermore, we exploited the translational invariance of the lattice.

A. Results given in the literature

The authors of Ref. [18] studied the behavior of the correlation function in the high-temperature phase of $O(N)$-invariant models in three dimensions by using perturbation theory, high-temperature series expansions, and the large-N expansion. They concluded that the leading cut contribution is associated with a three-particle state with $\mu_1 = 3m_1$. Furthermore, no bound state with a mass less than $3m_1$ should contribute. They arrived at the estimate

$$\lim_{t\searrow 0} \xi_{\mathrm{exp}}/\xi_{\mathrm{2nd}} = 1.000\,200(3) \tag{18}$$

for the Ising universality class, where t is the reduced temperature.

In the low-temperature phase, there should be a contribution from a cut characterized by $\mu_1 = 2m_1$. This has been computed by the author of [19] at the one-loop level of perturbation theory. This calculation was extended to two loops in [20].

Corresponding estimates are

$$\lim_{t\nearrow 0} \xi_{\rm exp}/\xi_{\rm 2nd} \approx 1.006\,52 \text{ (at one loop)} \quad \text{and} \quad 1.012\,66 \text{ (at two loops)}. \tag{19}$$

In [20], the correlation matrix of a large number of different observables was determined in a Monte Carlo simulation of the Ising model and the ϕ^4 model on the simple-cubic lattice. The analysis of these data has shown that there is a bound state with

$$m_2/m_1 = 1.83(3). \tag{20}$$

This result was confirmed by solving the Bethe-Salpeter equation for the ϕ^4 theory in three dimensions at the one-loop level of perturbation theory [21]. Correspondingly, we [7] find that the ratio

$$\lim_{t\nearrow 0} \xi_{\rm exp}/\xi_{\rm 2nd} = 1.020(5) \tag{21}$$

is larger than the estimates (19) obtained from perturbation theory.

On the critical isotherm, for symmetry reasons, we expect that, similar to the low-temperature phase, there is a cut characterized by $\mu_1 = 2m_1$. Taking the numerical results for the linear lattice size $L = 120$, given in Table 1 of Ref. [22], we get $\xi_{\rm exp}/\xi_{\rm 2nd} = 1.06(2)$. Note that the authors of Ref. [22] simulated the improved ϕ^4 model on the simple-cubic lattice. This result suggests that also for the critical isotherm there is a bound state with $m_2 < 2m_1$.

B. Analyzing our numerical results

Here we briefly summarize our preliminary study of $\bar{G}(r)$, which is the basis of our evaluation of the correlation length below. We fitted our numerical results for $\bar{G}(r)$ both in the low-temperature phase and for the critical isotherm with the *Ansatz*

$$\bar{G}(r) = \sum_{i=1}^{n} c_i \exp(-m_i r) \tag{22}$$

using $n = 2$ and 3. In the case of the low-temperature phase, we find for all values of β where we simulated at $m_2 \approx 1.8m_1$, consistent with Ref. [20]. Furthermore, $m_3 \approx 2.3m_1$. It is likely that this result is due to the cut at $2m_1$. Despite the high statistical accuracy that we reached here for $\bar{G}(r)$, we were not able to get more precise results for the ratio m_2/m_1 than that obtained in Ref. [20], analyzing the correlation matrix of several observables. Therefore, we shall not go into the details of our analysis.

For the critical isotherm, we find that $m_2 \approx 2.3m_1$. The results for m_3 depend very much on the range of r that is fitted. We conclude that there is no bound state with $m_2 < 2m_1$. The main deviations from a single exponential decay of $\bar{G}(r)$ are due to a cut with $\mu_1 = 2m_1$.

Below we shall use the effective correlation length to obtain our final estimates of the exponential correlation length. We shall take the effective correlation length at the distance $R = c\xi_{\rm eff}$, self-consistently.

In the high-temperature phase, $\xi_{\rm eff}$ converges very rapidly. We take $c = 2$, which should guarantee that systematical errors are small compared with the statistical ones. In the case of the low-temperature phase, we computed results for the two choices $c = 7$ and 9. To estimate the systematic error of our result for the exponential correlation length, due to contributions of states with higher masses, we assumed $m_2 = 1.8m_1$. Then, fitting with an *Ansatz* that contains two exponentials, we estimated the ratio of the two amplitudes. We obtained $c_2/c_1 \approx 0.04$ for the values of β we simulated at. Then, for this *Ansatz*, having inserted our numerical estimate for the amplitude ratio, we computed $\xi_{\rm eff}$. It turns out that the ratio $\xi_{\rm exp}/\xi_{\rm eff} \lessapprox 1.000\,12$ and $1.000\,024$ for $c = 7$ and 9, respectively.

In the case of the critical isotherm, we proceeded in a similar way, now assuming $m_2 = 2m_1$. Based on our analysis, we decided to take $c = 6$, where $\xi_{\rm exp}/\xi_{\rm eff} \lessapprox 1.000\,06$.

IV. CRITICAL BEHAVIOR AND UNIVERSAL AMPLITUDE RATIOS

In this section, we briefly summarize the results needed for the analysis of our numerical data. For a detailed discussion, see, for example, the review [23]. In the neighborhood of the critical point, various quantities diverge, following power laws. For example, the exponential and the second-moment correlation length at vanishing external field behave as

$$\xi_{\rm exp} \simeq f_{\rm exp,\pm}|t|^{-\nu}, \quad \xi_{\rm 2nd} \simeq f_{\rm 2nd,\pm}|t|^{-\nu}, \tag{23}$$

TABLE I. Results for the critical isotherm $\beta = 0.387\,721\,735$ of the Blume-Capel model at $D = 0.655$. In the first column, we give the value of the external field h. The second column contains the linear lattice size L. Next we give the number of update cycles divided by 10^5. It follows the magnetic susceptibility, computed by using the improved estimator. Then we give the results of the second-moment correlation length $\xi_{\rm 2nd}$ and the exponential correlation length $\xi_{\rm exp}$. It follows the magnetization m and the renormalization-group invariant quantity u, Eq. (32). The estimates given here for χ, $\xi_{\rm 2nd}$, and $\xi_{\rm exp}$ are computed using $R = 6\xi_{\rm eff}$, Eq. (17).

h	L	stat/10^5	χ	$\xi_{\rm 2nd}$	$\xi_{\rm exp}$	m	u
0.02	60	100	4.652 93(10)	1.467 172(38)	1.508 49(16)	0.454 389 8(13)	21.4066(13)
0.01	80	100	8.136 46(17)	1.948 550(48)	1.989 96(21)	0.393 999 0(12)	21.2536(13)
0.006	100	100	12.245 71(26)	2.398 411(59)	2.441 38(25)	0.354 480 6(11)	21.1909(12)
0.003	130	100	21.274 00(46)	3.176 033(80)	3.224 65(34)	0.306 965 4(11)	21.1415(13)
0.001	200	60	50.8996(15)	4.950 94(17)	5.016 44(69)	0.244 201 2(14)	21.0997(17)
0.0006	248	40	76.3007(27)	6.083 55(24)	6.1609(10)	0.219 532 8(16)	21.0950(20)
0.0002	380	19	182.140(10)	9.473 62(57)	9.5850(23)	0.174 569 2(21)	21.0884(30)
0.0001	500	16	315.267(20)	12.526 82(82)	12.6725(34)	0.151 055 7(23)	21.0864(32)

where $t = \beta_c - \beta$ is the reduced temperature. For simplicity, we skip the usual normalization $1/\beta_c$. $f_{\mathrm{exp},\pm}$ and $f_{\mathrm{2nd},\pm}$ are the amplitudes and $\pm$ indicates whether the high- (+) or the low-temperature phase (−) is considered. The critical exponent of the correlation length ν is the same for all systems in a given universality class. For a vanishing external field, the magnetization, the magnetic susceptibility, and the specific heat behave as

$$m \simeq B(-t)^{\beta}, \quad \chi \simeq C_{\pm}|t|^{-\gamma}, \quad C_h \simeq A_{\pm}|t|^{-\alpha}. \tag{24}$$

Note that here β is, as usual, the critical exponent of the magnetization. Also the behavior on the critical isotherm, $\beta = \beta_c$ and $h \neq 0$, is given by power laws. In the following, we assume $h > 0$. The exponential and the second-moment correlation length behave as

$$\xi_{\mathrm{exp}} \simeq f_{\mathrm{exp},c} h^{-\nu_c}, \quad \xi_{\mathrm{2nd}} \simeq f_{\mathrm{2nd},c} h^{-\nu_c}. \tag{25}$$

The magnetization and the magnetic susceptibility behave as

$$m \simeq B_c h^{1/\delta}, \quad \chi \simeq C_c h^{1/\delta - 1}. \tag{26}$$

The critical exponents ν, β, γ, α, ν_c, and δ are the same for all systems in a given universality class, which is in our case the universality of the Ising model in three dimensions. Following renormalization-group theory, the exponents listed above can be expressed in terms of only two exponents. For example, one could express them in terms of the so called RG exponents y_t and y_h, where the subscript t indicates a thermal perturbation and h denotes a perturbation by the external field:

$$\nu = 1/y_t, \quad \alpha = 2 - \frac{d}{y_t}, \quad \eta = d + 2 - 2y_h, \quad \beta = \frac{d - y_h}{y_t},$$
$$\gamma = \frac{2y_h - d}{y_t}, \tag{27}$$

and for the critical isotherm

$$\nu_c = 1/y_h, \quad \delta = \frac{y_h}{d - y_h}, \tag{28}$$

where d is the dimension of the system. Quite recently, Simmons-Duffin [24] computed the dimensions of the fields by using the conformal bootstrap with high precision,

$$3 - y_h = \Delta_\sigma = 0.518\,151(6), \quad 3 - y_t = \Delta_\epsilon = 1.412\,64(6). \tag{29}$$

These results are fully consistent with, but clearly more accurate than,

$$\nu = 0.630\,02(10), \quad \eta = 0.036\,27(10) \tag{30}$$

obtained by a finite-size scaling analysis of Monte Carlo data obtained for the improved Blume-Capel model [14]. For a comparison with the vast amount of results obtained by various methods, see [14,24]. Taking the results of [24], one arrives at $\nu = 0.629\,977(24)$, $\eta = 0.036\,302(12)$, $\gamma = 1.237\,084(54)$, $\beta = 0.326\,423(16)$, $\alpha = 0.110\,069(71)$, $\nu_c = 0.402\,925\,4(10)$, $\delta = 4.789\,818(67)$, and $1/\delta = 0.208\,776(3)$.

The $\simeq$ in the power laws listed above means that they are strictly valid only in the scaling limit $t \to 0$. At finite t, corrections have to be taken into account. For example, the magnetic susceptibility behaves as

$$\chi = C_{\pm}|t|^{-\gamma}\,(1 + a_{\pm}|t|^{-\theta} + bt + c_{\pm}|t|^{-\theta'} + \cdots) + d(t), \tag{31}$$

where $d(t)$ is the analytic background. The terms $a_{\pm}|t|^{-\theta}$ and $c_{\pm}|t|^{-\theta'}$ are singular or confluent corrections, while bt is an analytic or nonconfluent correction. Furthermore, $\theta = \nu\omega$ and $\theta' = \nu\omega'$. Various methods, e.g., the ϵ-expansion, perturbation theory in three dimensions fixed, high-temperature series expansion, and Monte-Carlo simulations of lattice models give consistently $\omega \approx 0.8$ for the exponent of the leading correction. For the analysis of our data, we shall use $\omega = 0.832(6)$ [14]. The authors of [25] obtained $\omega = \Delta_{\epsilon'} - 3 = 0.8303(18)$, which differs slightly from our central value. Note that in the case of the model studied here, the amplitude of leading corrections is small. Hence the precise value of ω has little influence on our final results.

There is a subleading correction due to the breaking of the Galilean invariance of space by the simple-cubic lattice. The associate correction exponent is $\omega'' \approx 2$. For a precise estimate, see [18].

Using the scaling field method, the authors of Ref. [26] find a subleading correction with the exponent $\omega' = 1.67(11)$. Up to now, there is no confirmation of this finding by using other methods. In the following numerical analysis we shall assume the existence of this correction, which has little influence on central values but enlarges the estimate of systematic errors.

With regard to physics results, we are mainly aiming at so called universal amplitude ratios that are characteristic for the universality class of the three-dimensional Ising model. While individual amplitudes depend on the microscopic details of the model, certain combinations are universal. The combinations of the corresponding quantities have a critical exponent that is equal to zero, which means that they are renormalization-group invariant or dimensionless. First, we compute the ratios of amplitudes $f_{\mathrm{exp},+}/f_{\mathrm{2nd},+}$, $f_{\mathrm{exp},-}/f_{\mathrm{2nd},-}$, and $f_{\mathrm{exp},c}/f_{\mathrm{2nd},c}$. The ratios $f_{\mathrm{2nd},+}/f_{\mathrm{2nd},-}$ and C_+/C_- relate the low- and high-temperature phase. For a broken $\mathbb{Z}_2$-symmetry we define the coupling

$$u = \frac{3\chi}{\xi_{\mathrm{2nd}}^3 m^2}. \tag{32}$$

For $h = 0$, in the low-temperature phase we get in the scaling limit

$$u^* = \lim_{t \nearrow 0} u(t,0) = \frac{3C_-}{f_{\mathrm{2nd},-}^3 B^2} \tag{33}$$

and analogously

$$u_c = \lim_{h \searrow 0} u(0,h) = \frac{3C_c}{f_{\mathrm{2nd},c}^3 B_c^2} \tag{34}$$

for the critical isotherm. The quantity

$$Q_2 = (f_{\mathrm{2nd},c}/f_{\mathrm{2nd},+})^{2-\eta}\, C_+/C_c \tag{35}$$

connects the critical isotherm with the high-temperature phase. Finally,

$$R_\chi = C_+ D_c B^{\delta - 1}, \tag{36}$$

where $h \simeq D_c m^{\delta}$ relates the critical isotherm with both the low- and the high-temperature phase.

V. THE SIMULATIONS

The exchange cluster algorithm is not ergodic on it own. Therefore, additional updates of the individual systems are performed. In particular, an update cycle is composed of the following:

(i) One sweep with the local heat bath algorithm for both systems.

(ii) Standard cluster updates of both systems.

(iii) One sweep with the local Todo-Suwa [27,28] algorithm for both systems.

(iv) One Swendsen-Wang exchange cluster update.

(v) Random translation of one system.

Due to a lack of time, we did not optimize this update cycle. Let us briefly discuss the choice of the cluster updates of the individual systems: In the low-temperature phase, we updated the individual systems by using the single-cluster algorithm. The number of single-cluster updates was chosen roughly as the total volume of the lattice divided by the average size of a cluster. In the high-temperature phase, we updated the individual systems by using the Swendsen-Wang algorithm. This allowed us to compare the variance-reduced estimators of the correlation function that are based on the standard Swendsen-Wang cluster algorithm and the Swendsen-Wang version of the exchange cluster algorithm.

In the case of the critical isotherm, the cluster algorithm applied to the individual systems has to be modified to take the external field into account [29,30]. The construction of the clusters is the same as for a vanishing external field $h = 0$. Following Ref. [29], there are two ways to incorporate the external field. The first one is by representing the external field by a "ghost-spin." The link of a spin s_x with the ghost-spin is frozen with the probability

$$p_{f,h} = 1 - p_{d,h}, \tag{37}$$

where the delete probability $p_{d,h} = \min[1, \exp(-2hs_x)]$. All clusters that are frozen to the ghost-spin keep the old sign of the spins. A cluster is frozen to the ghost-spin if it contains at least one spin that is frozen to the ghost-spin. Clusters that are not frozen to the ghost-spin get the sign plus or minus with equal probability.

The alternative is to chose the new sign of the clusters with the heat-bath probability

$$p_C(-) = \frac{\exp\left(-h\sum_{x\in C} s_x\right)}{\exp\left(-h\sum_{x\in C} s_x\right) + \exp\left(h\sum_{x\in C} s_x\right)} \tag{38}$$

and $p_C(+) = 1 - p_C(-)$.

Here we used a modified version of the ghost-spin variant. First we run through all sites of the lattice and decide whether the spin is frozen to the ghost-spin or not. Then we construct all clusters that contain spins that are frozen to the ghost-spin. As in Ref. [29], these clusters keep their sign. In contrast to [29], we change the sign of all clusters that are not frozen to the ghost-spin. This has the technical advantage that we need not construct these clusters, since we just have to change the sign of all spins that do not belong to clusters that are frozen to the ghost-spin. A preliminary study shows that also autocorrelation times compare favorably. In our update cycle, we performed one of these updates for each system.

We used the SIMD-oriented Fast Mersenne Twister algorithm [31] as a pseudo-random-number generator. In total, all our simulations took about 18 years of CPU time on a single core of an Intel(R) Xeon(R) E5-2660 v3 running at 2.60 GHz.

A. The critical isotherm

We simulated at the estimate of the inverse critical temperature $\beta = 0.387\,721\,735$ at various values of the external field. Preliminary simulations indicate that the deviation from the thermodynamic limit for the quantities that we study is below our statistical accuracy for $L \gtrapprox 11\xi$. Since the variance-reduced estimators studied here are self-averaging, we decided to simulate much larger lattices. Here, by self-averaging we simply mean that for $L \gg \xi$ the variance is inversely proportional to the volume L^3. Our final results, which are given in Table I, are taken from simulations with $L \approx 40\xi$.

First, let us discuss the performance of the improved estimator of the two-point function. Actually, we did not directly determine the variance of the quantities. During the simulation we computed the averages over bins of 1000 measurements each. Hence we only had access to the statistical error and not to the variance and the autocorrelation times separately. The statistical errors are computed by using the jackknife method throughout. Analyzing the data for the standard estimator of the slice-slice correlation function, we find that the statistical error depends little on the distance between the slices. Hence for the connected slice-slice correlation function, the relative statistical error increases proportional to $\exp(r/\xi_{\rm exp})$. The same holds for the effective correlation length $\xi_{\rm eff}$ computed from the standard estimator of the slice-slice correlation function. On the contrary, we find for all values of the external field h that the statistical error of the variance-reduced estimator of the slice-slice correlation function decreases as $\exp(-r/[2\xi_{\rm exp}])$. Hence the relative statistical error increases as $\exp(r/[2\xi_{\rm exp}])$. The same holds for the effective correlation length $\xi_{\rm eff}$ computed from the variance-reduced estimator of the slice-slice correlation function.

Now let us turn to the analysis of our data. First, we fitted our data for the second-moment correlation length, the magnetization, and the magnetic susceptibility using power-law *Ansätze*. Then we studied universal ratios that consist of quantities defined on the critical isotherm only.

We fitted the second-moment correlation length with the *Ansätze*

$$\xi_{\rm 2nd} = f_{\rm 2nd,c} h^{-\nu_c} \left(1 + \sum_i^n a_i h^{\epsilon_i}\right), \tag{39}$$

where $f_{\rm 2nd,c}$ and the a_i are the free parameters of the fit. We performed fits for $n = 1$, 2, and 3 using different choices for the correction exponents ϵ_i. As values we have used $\epsilon_i = 0.832\nu_c$, $1.67\nu_c$, $2\nu_c$, and 2, with $\nu_c = 0.402\,925\,4$. Only for the exponent $\epsilon = 2\nu_c$ we find an amplitude that is clearly different from zero. In particular, fitting the data with a single correction term and $\epsilon_1 = 2\nu_c$, we find $f_{\rm 2nd,c} = 0.306\,321(17)$, $a_1 = -0.161(18)$, and $\chi^2/{\rm d.o.f.} = 0.12$ (where d.o.f. denotes degrees of freedom). Our final estimate, and in particular the error bar, is chosen such that the results of various plausible fits are accommodated. To obtain the dependence of the central value on ν_c and β_c, we repeated a selection of fits for slightly

shifted values of ν_c and β_c. We arrive at

$$f_{2\mathrm{nd},c} = 0.306\,31(18) - 220\ (\beta_c - 0.387\,721\,735) - 3\ (\nu_c - 0.402\,925\,4). \quad (40)$$

Next we fitted the magnetization with the *Ansätze*

$$m = B_c\, h^{1/\delta}\left(1 + \sum_i^n a_i h^{\epsilon_i}\right) \quad (41)$$

using $n = 1$ and 2. It turns out that for $n = 1$ and $\epsilon_1 = 2\nu_c$, we get $\chi^2/\mathrm{d.o.f.} = 0.68$ taking all our values of h into account. One gets $B_c = 1.033\,400\,69(28)$ and $a_1 = -0.114\,79(10)$. To get an estimate of possible systematic errors due to further corrections, we performed fits with $n = 2$, adding a term with a correction exponent $\epsilon_2 = 0.832\nu_c$ or $\epsilon_2 = 1.67\nu_c$. In both cases, the amplitudes of the corresponding corrections remain compatible with zero within the error bars. In particular for the fit with $\epsilon_2 = 0.832\nu_c$, the statistical error of B_c increases considerably compared with $n = 1$ and $\epsilon_1 = 2\nu_c$. We quote

$$B_c = 1.033\,401(20) + 170\ \ (\beta_c - 0.387\,721\,735) + 7\ \ (1/\delta - 0.208\,776) \quad (42)$$

as our final result. Next we have analyzed the magnetic susceptibility. Also here we find that all data can be fitted well with an *Ansatz* that contains a single correction term with the correction exponent $\epsilon = 2\nu_c$. In particular, we find $\chi^2/\mathrm{d.o.f.} = 0.89$ and $C_c = 0.215\,748\,7(34)$ and $a_1 = -0.558\,05(66)$. As in the case of the magnetization we performed fits, where we added a second correction term. We arrive at our final estimate

$$C_c = 0.215\,749(15) + 73\ (\beta_c - 0.387\,721\,735) + 1.5\ (1/\delta - 0.208\,776). \quad (43)$$

The amplitudes of the magnetization and the magnetic susceptibility on the critical isotherm are trivially related by $C_c = B_c/\delta$. Our numerical estimates of C_c and B_c are indeed consistent with this relation.

Next we analyzed the renormalization-group invariant quantity u, Eq. (32). We used the *Ansatz*

$$u = u_c + c_1 \xi_{2\mathrm{nd}}^{-\epsilon_1} + c_2 \xi_{2\mathrm{nd}}^{-\epsilon_2}, \quad (44)$$

where u_c, c_1, and c_2 are the free parameters. We performed fits using $\epsilon_1 = 0.832$, which is our estimate of ω and the two choices $\epsilon_2 = 2\omega$ and $\epsilon_2 = 2$.

For both choices we get an acceptable $\chi^2/\mathrm{d.o.f.}$ taking into account all data except for our largest value of h. As our final result, we take

$$u_c = 21.086(20), \quad (45)$$

which is the value of u for our smallest value of h. The error bar is taken such that the results of the fits discussed above are covered. In Fig. 1 we plot our estimate of $\xi_{\mathrm{exp}}/\xi_{2\mathrm{nd}}$ along with its corrected counterpart $z_{\mathrm{cor}}\xi_{\mathrm{exp}}/\xi_{2\mathrm{nd}}$ as a function of ξ_{exp}^{-2}. We see that at least for the smaller values of the correlation length the major part of the corrections is indeed eliminated by multiplying with z_{cor}. The fact that the data for $\xi_{\mathrm{exp}}/\xi_{2\mathrm{nd}}$ fall more or less on a straight line reflects that $z_{\mathrm{cor}} - 1 = O(\xi_{\mathrm{exp}}^{-2})$. An analysis similar to that of the quantity u above results in

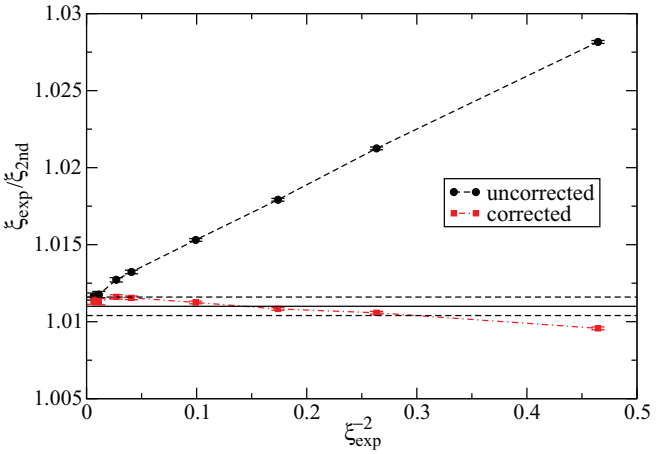

FIG. 1. We plot $\xi_{\mathrm{exp}}/\xi_{2\mathrm{nd}}$ along with its corrected counterpart $z_{\mathrm{cor}}\xi_{\mathrm{exp}}/\xi_{2\mathrm{nd}}$ for the critical isotherm as a function of ξ_{exp}^{-2}. The dashed lines connecting the data points are there to guide the eye. Note that the symbols for the two smallest values of h partially overlap. The solid horizontal line gives our estimate for the scaling limit. The dashed lines parallel to it indicate its error.

$f_{\mathrm{exp},c}/f_{2\mathrm{nd},c} = 1.0109(5)$. As our final estimate, we quote

$$f_{\mathrm{exp},c}/f_{2\mathrm{nd},c} = 1.0110(6). \quad (46)$$

This estimate also includes the results for $z_{\mathrm{cor}}\xi_{\mathrm{exp}}/\xi_{2\mathrm{nd}}$ obtained for our two smallest values of h.

B. The low-temperature phase, $h = 0$

First we studied finite-size effects at $\beta = 0.391$ and 0.42 by simulating a large range of lattice sizes. Throughout we performed 10^8 update cycles. At the level of our statistical accuracy, the results for the correlation length, the magnetic susceptibility, the magnetization, and the energy density are consistent among each other for $L \geqslant 12$ and 48 for $\beta = 0.42$ and 0.391, respectively. Taking our final results $\xi_{\mathrm{exp}} = 1.087\,01(35)$ and 4.4449(19), discussed below, we find consistently that for $L \gtrapprox 11\xi_{\mathrm{exp}}$ deviations from the thermodynamic limit are small compared with our statistical errors. Furthermore, the numerical results are consistent with an approach of the thermodynamic limit that is exponentially fast in the linear lattice size. Concerning the validity of the variance-reduced estimator, we checked whether the signs of P and M_1M_2 coincide. For $\beta = 0.42$, we find that this is the case for the fraction 0.980 740(46), 0.998 769(12), and 0.999 982 3(14) of pairs of configurations for the linear lattice sizes $L = 4$, 6, and 8, respectively. For the larger lattice sizes $L = 10, 12, 16, \ldots$ that we simulated, the sign of P and M_1M_2 coincides for all configurations that we analyzed. For $\beta = 0.391$, we find a fraction of 0.999 972(18) for $L = 32$, while for all larger lattice sizes that we simulated, the sign of P and M_1M_2 coincides for all configurations that we analyzed. Furthermore, the analysis of our data shows that the variance-reduced estimator of the correlation function is self-averaging.

Our final estimates are obtained for lattice sizes $L \gtrapprox 44\xi_{\mathrm{exp}}$, where deviations from the thermodynamic limit are much

TABLE II. Results for the low-temperature phase of the Blume-Capel model at $D = 0.655$ and a vanishing external field $h = 0$. In the first column, we give the inverse temperature β. The second column contains the linear lattice size L. Next we give the number of update cycles divided by 10^5. Then we present the magnetic susceptibility, computed by using the improved estimator. Then we give the results of the second-moment correlation length ξ_{2nd} and the exponential correlation length ξ_{exp}. The corrected ratio $z_{cor}\xi_{exp}/\xi_{2nd}$ follows, as well as the renormalization-group invariant quantity u, Eq. (32). All estimates given here are computed for $R = 7\xi_{eff}$, Eq. (17).

β	L	stat/10^5	χ	ξ_{2nd}	ξ_{exp}	$z_{cor}\,\xi_{exp}/\xi_{2nd}$	u
0.42	48	205	1.964992(32)	1.031143(20)	1.08696(14)	1.01786(12)	14.07096(67)
0.41	60	126	3.193168(68)	1.302022(33)	1.35761(21)	1.01949(14)	14.06315(84)
0.40	88	100	6.84022(17)	1.892267(52)	1.95348(33)	1.02116(16)	14.06400(91)
0.396	112	104	11.24176(28)	2.423518(68)	2.49420(41)	1.02230(15)	14.06351(91)
0.394	132	100	15.89635(42)	2.883053(83)	2.96210(51)	1.02256(16)	14.06513(93)
0.393	148	100	19.74238(52)	3.214815(90)	3.30138(55)	1.02301(16)	14.06754(91)
0.392	168	102	25.65302(69)	3.66821(11)	3.76268(63)	1.02274(16)	14.07048(93)
0.391	196	101	35.73272(97)	4.33667(13)	4.44557(75)	1.02295(16)	14.07045(93)
0.39	248	100	56.1525(15)	5.45174(16)	5.58651(95)	1.02335(16)	14.07095(92)
0.389	400	33	114.9821(48)	7.84194(34)	8.0305(20)	1.02338(23)	14.0755(14)
0.3883	580	10	307.102(26)	12.9205(12)	13.2266(72)	1.02345(51)	14.0771(29)

smaller than our statistical errors. Our numerical estimates are summarized in Table II.

Similar to the critical isotherm, we did not analyze autocorrelation times and variance separately. Instead, we computed the statistical error using a jackknife analysis. For the standard estimator of the slice-slice correlation function $\bar{G}(r)$ we find that the statistical error is virtually independent of the distance r. Hence the signal-to-error ratio decreases as $\exp(-r/\xi_{exp})$. In contrast, for the variance-reduced estimator we find that the statistical error decreases as $\exp(-r/[2\xi_{exp}])$. Hence the signal-to-error ratio decreases as $\exp(-r/[2\xi_{exp}])$. Similar observations hold for the effective correlation length $\xi_{eff}(r)$, which is computed from $\bar{G}(r)$. This improvement allowed us to take $\xi_{eff}(r)$ at about twice the distance compared with Ref. [7] as an estimate of ξ_{exp}, making systematical errors negligible.

We analyzed the data for the magnetization obtained here along with those of Ref. [7] by using *Ansätze* of the type

$$m = B\,(-t)^{\beta}\left(1 + \sum_{i}^{n} a_i\,(-t)^{\epsilon_i}\right) \tag{47}$$

with $t = \beta_c - \beta$. We performed fits for $n = 2$ and 3. We fixed the exponents $\beta = 0.326\,423$, $\epsilon_1 = 0.832\nu$, $\epsilon_2 = 1$, and $\epsilon_3 = 2\nu$, where $\nu = 0.629\,977$. For $n = 3$ we get χ^2/d.o.f. close to 1 up to $\beta_{max} = 0.41$, where we take all data for $\beta \leqslant \beta_{max}$ into account. For fits with $n = 2$ we get χ^2/d.o.f. up to about $\beta_{max} = 0.395$. Comparing the results of different fits, we arrive at the final estimate,

$$\begin{aligned} B = {} & 1.9875(3) + 2460\,(\beta_c - 0.387\,721\,735) \\ & + 22\,(\beta - 0.326\,423). \end{aligned} \tag{48}$$

In the case of the coupling u, we abstain from fitting, since there is little variation with β. As a final estimate, we take the value obtained for our smallest value of β,

$$u^* = 14.08(1). \tag{49}$$

The error bar is chosen such that also the results for $\beta = 0.389$ and 0.39 are covered. This result is fully consistent, but more precise than our previous estimate $u^* = 14.08(5)$ [7]. For a comparison with results obtained by using other methods and previous Monte Carlo simulations, see Ref. [7].

Also in the case of $z_{cor}\xi_{exp}/\xi_{2nd}$ we abstain from fitting. As our final estimate, we take

$$f_{exp,-}/f_{2nd,-} = 1.0234(6), \tag{50}$$

where the error bar is chosen such that the results for our four smallest values of β are covered. For all values of β, we compared our result for $z_{cor}\xi_{exp}/\xi_{2nd}$ using $R = 7\xi_{eff}$ and $R = 9\xi_{eff}$, Eq. (17). We conclude that the difference should be clearly smaller than the error bar given in Eq. (50). Our present result is consistent with, but more precise than, $f_{exp,-}/f_{2nd,-} = 1.020(5)$ obtained in Ref. [7]. For a comparison with results obtained by using other methods and previous Monte Carlo simulations, see Ref. [7].

C. The high-temperature phase

Finally, we also performed simulations in the high-temperature phase. We simulated at values of the inverse temperature $\beta_h = 2\beta_c - \beta_l$, where $\beta_c = 0.387\,721\,735$ is our estimate of the inverse critical temperature and β_l are the values of β that are used in Sec. V B. The linear lattices sizes L are essentially the same as for the corresponding values of β in the low-temperature phase.

We computed variance-reduced estimators both based on the standard Swendsen-Wang update and the cluster exchange update of the two systems. In the following, $\bar{G}_{SW}(r)$ and $\bar{G}_{EC}(r)$ denote the results for $\bar{G}(r)$ obtained from the two estimators, respectively. We find that the ratio of the statistical errors of $\bar{G}_{EC}(r)$ and $\bar{G}_{SW}(r)$ depends little on r. In both cases, we find that the ratio of signal to statistical error decreases as $\exp(-r/[2\xi_{exp}])$. The same holds for the effective correlation length obtained from $\bar{G}_{SW}(r)$ and $\bar{G}_{EC}(r)$. For large distances, we find for all values of β that we simulated a ratio of about 1.55 between the statistical errors of $\bar{G}_{EC}(r)$ and $\bar{G}_{SW}(r)$. For small distances, we see a smaller factor that depends slightly on β. For our smallest β, we find a factor of about 1.5 that decreases to about 1.2 for our largest value of β. Note that in the case of $\bar{G}_{SW}(r)$, the measurements of both systems enter.

TABLE III. Results for the high-temperature phase of the Blume-Capel model at $D = 0.655$. We give results for the same quantities as in Table II for the low-temperature phase. Only u is missing, since it is not defined for a vanishing magnetization. All estimates given here are computed for $R \approx 2\xi_{\rm eff}$, Eq. (17). The numbers are obtained from improved estimators based on the standard Swendsen-Wang algorithm.

β	L	stat/10^5	χ	$\xi_{\rm exp}$	$\xi_{\rm 2nd}$	$z_{\rm cor}\xi_{\rm exp}/\xi_{\rm 2nd}$
0.35544347	48	150	10.15694(17)	1.923431(29)	1.944827(36)	1.0000705(45)
0.36544347	64	112	16.00107(29)	2.456110(40)	2.473081(49)	1.0000823(43)
0.37544347	88	107	33.28360(75)	3.611554(68)	3.623445(79)	1.0001157(40)
0.37944347	112	105	54.0942(13)	4.647652(90)	4.65721(10)	1.0001348(40)
0.38144347	132	111	76.0765(19)	5.54245(11)	5.55076(13)	1.0001459(41)
0.38244347	148	101	94.2427(25)	6.18851(13)	6.19619(15)	1.0001546(40)
0.38344347	168	101	122.1430(34)	7.07068(15)	7.07771(18)	1.0001625(42)
0.38444347	196	101	169.6870(59)	8.36931(19)	8.37571(22)	1.0001700(45)
0.38544347	248	80	266.0115(91)	10.53510(27)	10.54096(30)	1.0001809(47)
0.38644347	400	28	543.398(29)	15.17511(58)	15.18080(65)	1.0001944(66)
0.38714347	580	12	1449.01(15)	25.0266(18)	25.0332(20)	1.000199(12)

Hence the performance of the two variance-reduced estimators is very similar. Results for various quantities derived from $\bar{G}_{\rm SW}(r)$ are summarized in Table III.

We analyzed the data for the second-moment correlation length given here along with those of Ref. [32]. We used *Ansätze* of the type

$$\xi_{\rm 2nd} = f_{\rm 2nd,+} t^{-\nu} \left(1 + \sum_i^n a_i t^{\epsilon_i} \right) \tag{51}$$

with $n = 2$ and 3. The reduced temperature is $t = \beta_c - \beta$. Free parameters are $f_{\rm 2nd,+}$ and a_i. We fixed $\nu = 0.629\,977$ and the correction exponents $\epsilon_1 = 0.832\nu$, $\epsilon_2 = 1$, and $\epsilon_3 = \gamma \approx 2\nu$. Taking into account the results of various fits, we arrive at

$$\begin{aligned} f_{\rm 2nd,+} &= 0.2284(1) - 2.1\ (\nu - 0.629\,977) \\ &\quad + 500\ (\beta_c - 0.387\,721\,735). \end{aligned} \tag{52}$$

In a similar way, we arrive at the estimate of the amplitude of the magnetic susceptibility

$$\begin{aligned} C_+ &= 0.143\,00(5) - 1.2\ (\gamma - 1.237\,084) \\ &\quad + 300\ (\beta_c - 0.387\,721\,735). \end{aligned} \tag{53}$$

Next we studied amplitude ratios that combine the high- with the low-temperature phase. Following [7,33], we computed the ratios $R_\chi(\beta_l - 0.387\,721\,735) = \chi(2 \times 0.387\,721\,735 - \beta_l)/\chi(\beta_l)$ and $R_{\xi_{\rm 2nd}}(\beta_l - 0.387\,721\,735) = \xi_{\rm 2nd}(2 \times 0.387\,721\,735 - \beta_l)/\xi_{\rm 2nd}(\beta_l)$. In this way, the divergence is canceled and the value of the critical exponent is not needed. We fitted these two quantities with the *Ansätze*

$$R(t) = R^* + a_1 t^{\epsilon_1} + a_2 t \tag{54}$$

and

$$R(t) = R^* + a_1 t^{\epsilon_1} + a_2 t + c t^{\epsilon_3}, \tag{55}$$

where we take $\epsilon_1 = \nu\omega$ and $\epsilon_3 = \gamma \approx 2\nu$. To obtain the dependence of our result on the value of β_c, we repeated the analysis, assuming $\beta_c = 0.387\,727\,6$, which is our central estimate of β_c plus the error bar. Our final estimates are

$$\frac{C_+}{C_-} = 4.714(4) + 36\,000\ (\beta_c - 0.387\,721\,735) \tag{56}$$

and

$$\frac{\xi_{\rm 2nd,+}}{\xi_{\rm 2nd,-}} = 1.940(2) + 11\,000\ (\beta_c - 0.387\,721\,735). \tag{57}$$

These results are consistent with $\frac{C_+}{C_-} = 4.713(7)$ and $\frac{\xi_{\rm 2nd,+}}{\xi_{\rm 2nd,-}} = 1.939(5)$ given in [7]. For a detailed comparison with estimates obtained in the literature, see [7].

To get the universal amplitude ratio Q_2, we first analyzed

$$r = \chi/\xi_{\rm 2nd}^{2-\eta} \tag{58}$$

both for the high-temperature phase as well as the critical isotherm. We fitted our data with the *Ansatz*

$$r = r_\infty + a_1 \xi_{\rm 2nd}^{-\epsilon_1} + a_2 \xi_{\rm 2nd}^{-\epsilon_2}, \tag{59}$$

where r_∞, a_1, and a_2 are the free parameters of the fit. We fixed $\epsilon_1 = 0.832$ and $\epsilon_2 = 1.67$ or 2. In the case of the high-temperature phase, the fits with $\epsilon_2 = 1.67$ are clearly better than those with $\epsilon_2 = 2$. Comparing the results of different fits, we arrive at $r_{\infty,\rm high} = 2.5960(15)$ for the high-temperature phase. Here we have also taken into account the uncertainty of η. In the case of the critical isotherm, we arrive at $r_{\infty,c} = 2.2020(20)$. As our result for the universal amplitude ratio, we quote

$$Q_2 = r_{\infty,\rm high}/r_{\infty,c} = 1.179(2). \tag{60}$$

This can be compared with $Q_2 = 1.201(10)$ and 1.195(10) obtained in Refs. [22] and [34], respectively. For a comprehensive collection of results obtained by various methods, see Tables 11 and 12 of the review [23].

Finally, using the amplitudes computed above,

$$R_\chi = C_+ D_c B^{\delta-1} = 1.650(3). \tag{61}$$

This result can be compared with $R_\chi = 1.723(13)$ obtained from Monte Carlo simulations of the improved ϕ^4 model on the simple-cubic lattice [22], and $R_\chi = 1.660(4)$ using high-temperature series expansions of improved lattice models in combination with a parametric representation of the equation of state [34]. For results obtained by other methods, see Table 12 of the review [23].

VI. CONCLUSIONS AND OUTLOOK

We discussed a variance-reduced estimator of the connected two-point function that is based on the exchange cluster algorithm [8–10]. We studied the properties of this estimator at the example of the improved Blume-Capel model on the simple-cubic lattice. We performed simulations for the high- and low-temperature phase at a vanishing external field and for the critical isotherm. In the high-temperature phase, we find that the variance-reduced estimator of the slice-slice correlation function $\bar{G}(r)$ based on the standard Swendsen-Wang algorithm [1] and on the Swendsen-Wang version of the exchange cluster algorithm perform similarly. In both cases, the relative statistical error increases as $\exp(r/[2\xi_{\rm exp}])$. This is a clear improvement compared with $\exp(r/\xi_{\rm exp})$ for the standard estimator. The exchange cluster improved estimator still works in the presence of a broken $\mathbb{Z}_2$-symmetry. For the critical isotherm as well as the low-temperature phase, we find that the relative statistical error increases as $\exp(r/[2\xi_{\rm exp}])$, as is the case in the high-temperature phase. Analyzing the slice-slice correlation function, we confirm that for the low-temperature phase there is a second isolated exponentially decaying term with $\xi_2 \approx \xi_{\rm exp}/1.83$ [20,21]. In contrast, for the critical isotherm, we do not find such a contribution. The reduced statistical error allowed us to take the effective correlation length at a large separation of the slices as an estimate of the exponential correlation length $\xi_{\rm exp}$, reducing systematical errors to one-eighth of a per mille or less. This allows us to compute the ratio $f_{\rm exp}/f_{\rm 2nd}$ of the amplitudes of the exponential and the second-moment correlation length with high precision. Using our data for the magnetization, the magnetic susceptibility, and the correlation length, we computed various universal amplitude ratios. We compared our estimates with those of Refs. [7,22,34]. For a comprehensive review of results obtained by various methods, see Ref. [23].

It seems plausible that the variance-reduced estimator discussed here is also effective for other models with $\mathbb{Z}_2$ symmetry. However, it is quite unclear how the idea can be generalized to problems with another symmetry. In our assessment, the main virtue of the exchange cluster algorithm is the construction of variance-reduced estimators of excess quantities related to defects of various kinds in Ising-like systems. In Refs. [12,13], we computed the thermodynamic Casimir force using such an estimator.

ACKNOWLEDGMENTS

This work was supported by the DFG under Grant No. HA 3150/3-1.

APPENDIX: THE ISING MODEL ON THE CRITICAL ISOTHERM

We simulated the Ising model at $\beta = 0.221\,654\,62$, which is the estimate of the inverse critical temperature given in Eq. (A2) of [32]. We performed these simulations before we became aware of the variance-reduced estimators discussed in the main body of the text. We simulated lattices with $L_0 > L = L_1 = L_2$. Therefore, we computed the slice-slice correlation function in the 0 direction only. Also the ratio L/ξ is smaller than in our study of the improved Blume-Capel model. However, L is large enough to ignore deviations from the thermodynamic limit. Our results for the energy density $E = \frac{1}{L_0 L^2}\langle \sum_{\langle xy\rangle} s_x s_y\rangle$, the magnetization, the magnetic susceptibility, the second-moment correlation length, and the dimensionless quantity u are summarized in Table IV. All estimates given here are computed for $R \approx 4\xi_{\rm eff}$, Eq. (17). Therefore, we do not quote an estimate of $\xi_{\rm exp}$.

We fitted the data with similar *Ansätze* to those for the improved Blume-Capel model in the main body of the text. We fitted the magnetization with *Ansätze* of the form

$$m = B_c\, h^{1/\delta}\left(1 + \sum_{i=1}^{n} a_i h^{\epsilon_i}\right), \tag{A1}$$

where we fixed $1/\delta$ and the correction exponents ϵ_i. The free parameters of the fit are B_c and a_i. We used $\epsilon_1 = 0.832\nu_c$, $\epsilon_2 = 1.664\nu_c$ or $2\nu_c$, and $\epsilon_3 = 1$. For the *Ansatz* with $n = 1$ we get an acceptable χ^2/d.o.f. only when discarding most of the data points. Taking into account $h = 0.001$, 0.0006, and 0.00033 we get χ^2/d.o.f. $= 1.56$, $B_c = 1.395\,500(55)$, and $a_1 = -0.2066(4)$. Next we performed fits with $n = 2$ correction terms. Among our different choices, the smallest χ^2/d.o.f. are found for $\epsilon_2 = 1.664\nu_c$. Here we get, taking $h = 0.01$ down to 0.000 33 into account, χ^2/d.o.f. $= 1.40$, $B_c = 1.394\,070(34)$, $a_1 = -0.1825(3)$, and $a_2 = -0.1413(11)$. Finally, for $n = 3$, with $\epsilon_2 = 1.664\nu_c$ and $\epsilon_3 = 1$, we get χ^2/d.o.f. $= 1.40$ taking all values of h. The results for the free parameters of the fit are $B_c = 1.393\,971(39)$, $a_1 = -0.1806(5)$, $a_2 = -0.166(4)$, and $a_3 = 0.043(6)$.

TABLE IV. Results for the critical isotherm $\beta = 0.221\,654\,62$ of the standard Ising model on the simple-cubic lattice. For a discussion, see the text.

h	$L_0 \times L^2$	stat/10^6	E	m	χ	$\xi_{\rm 2nd}$	u
0.05	32×12^2	200	1.6576621(58)	0.6819794(16)	2.32857(15)	0.83556(24)	25.748(21)
0.02	48×20^2	200	1.4119028(37)	0.5794070(14)	5.33012(35)	1.25521(37)	24.085(20)
0.01	64×24^2	200	1.2833057(31)	0.5087991(15)	9.69650(64)	1.68910(41)	23.318(16)
0.005	100×36^2	113	1.1921108(26)	0.4450808(16)	17.3802(15)	2.26080(81)	22.778(23)
0.002	160×50^2	59	1.1124843(25)	0.3714069(21)	37.0357(45)	3.30542(16)	22.303(30)
0.001	160×68^2	45	1.0735366(24)	0.3231855(26)	65.174(11)	4.4007(28)	21.965(39)
0.0006	200×82^2	31	1.0529398(24)	0.2914486(31)	98.538(21)	5.4172(42)	21.892(48)
0.00033	300×100^2	27	1.0351784(19)	0.2580626(30)	159.599(34)	6.9184(55)	21.712(48)

Based on these fits, we arrive at our final estimate,

$$B_c = 1.3941(6), \quad a_1 = -0.19(2). \tag{A2}$$

Performing similar fits, we arrive at

$$f_{2\mathrm{nd},c} = 0.2771(12) \tag{A3}$$

for the amplitude of the second-moment correlation length. We analyzed our data for the coupling u by fitting with the *Ansatz* (44). We arrive at

$$u_c = 21.05(15), \tag{A4}$$

which is consistent with our result (45) obtained from the data for the improved Blume-Capel model.

[1] R. H. Swendsen and J.-S. Wang, Nonuniversal Critical Dynamics in Monte Carlo Simulations, Phys. Rev. Lett. **58**, 86 (1987).

[2] U. Wolff, Collective Monte Carlo Updating for Spin Systems, Phys. Rev. Lett. **62**, 361 (1989).

[3] U. Wolff, Monte Carlo simulation of a lattice field theory as correlated percolation, Nucl. Phys. B **300**, 501 (1988).

[4] M. Hasenbusch, Improved estimators for a cluster updating of $O(n)$ spin models, Nucl. Phys. B **333**, 581 (1990).

[5] U. Wolff, Asymptotic freedom and mass generation in the $O(3)$ nonlinear σ-model, Nucl. Phys. B **334**, 581 (1990).

[6] M. Hasenbusch, A Monte Carlo study of the three-dimensional XY universality class: Universal amplitude ratios, J. Stat. Mech.: Theor. Exp. (2008) P12006.

[7] M. Hasenbusch, Universal amplitude ratios in the three-dimensional Ising universality class, Phys. Rev. B **82**, 174434 (2010).

[8] O. Redner, J. Machta, and L. F. Chayes, Graphical representations and cluster algorithms for critical points with fields, Phys. Rev. E **58**, 2749 (1998).

[9] L. Chayes, J. Machta, and O. Redner, Graphical representations for Ising systems in external fields, J. Stat. Phys. **93**, 17 (1998).

[10] J. R. Heringa and H. W. J. Blöte, Geometric cluster Monte Carlo simulation, Phys. Rev. E **57**, 4976 (1998).

[11] J. Machta, M. E. J. Newman, and L. B. Chayes, Replica-exchange algorithm and results for the three-dimensional random field Ising model, Phys. Rev. E **62**, 8782 (2000).

[12] M. Hasenbusch, Thermodynamic Casimir forces between a sphere and a plate: Monte Carlo simulation of a spin model, Phys. Rev. E **87**, 022130 (2013).

[13] M. Hasenbusch, Thermodynamic Casimir effect in films: The exchange cluster algorithm, Phys. Rev. E **91**, 022110 (2015).

[14] M. Hasenbusch, A finite size scaling study of lattice models in the 3D Ising universality class, Phys. Rev. B **82**, 174433 (2010).

[15] F. Schmitz, P. Virnau, and K. Binder, Logarithmic finite-size effects on interfacial free energies: Phenomenological theory and Monte Carlo studies, Phys. Rev. E **90**, 012128 (2014).

[16] M. Hasenbusch, Monte Carlo studies of the three-dimensional Ising model in equilibrium, Int. J. Mod. Phys. C **12**, 911 (2001).

[17] M. E. Peskin and D. V. Schroeder, *An Introduction to Quantum Field Theory*, Addison-Wesley Advanced Book Program (Addison-Wesley, Reading, MA, 1995).

[18] M. Campostrini, A. Pelissetto, P. Rossi, and E. Vicari, The two point correlation function of three-dimensional O(N) models: Critical limit and anisotropy, Phys. Rev. E **57**, 184 (1998).

[19] P. Provero, Interaction effects in the spectrum of the three-dimensional Ising model, Phys. Rev. E **57**, 3861 (1998).

[20] M. Caselle, M. Hasenbusch, and P. Provero, Nonperturbative states in the 3-D ϕ^4 theory, Nucl. Phys. B **556**, 575 (1999).

[21] M. Caselle, M. Hasenbusch, P. Provero, and K. Zarembo, Bound states and glueballs in three-dimensional Ising systems, Nucl. Phys. B **623**, 474 (2002).

[22] J. Engels, L. Fromme, and M. Seniuch, Numerical equation of state and other scaling functions from an improved three-dimensional Ising model, Nucl. Phys. B **655**, 277 (2003).

[23] A. Pelissetto and E. Vicari, Critical phenomena and renormalization-group theory, Phys. Rep. **368**, 549 (2002).

[24] D. Simmons-Duffin, A semidefinite program solver for the conformal bootstrap, J. High Energy Phys. 06 (2015) 174.

[25] S. El-Showk, M. F. Paulos, D. Poland, S. Rychkov, D. Simmons-Duffin, and A. Vichi, Solving the 3d Ising model with the conformal bootstrap II. c-minimization and precise critical exponents, J. Stat. Phys. **157**, 869 (2014).

[26] K. E. Newman and E. K. Riedel, Critical exponents by the scaling-field method: The isotropic N-vector model in three dimensions, Phys. Rev. B **30**, 6615 (1984).

[27] S. Todo and H. Suwa, Geometric allocation approaches in Markov chain Monte Carlo, J. Phys.: Conf. Ser. **473**, 012013 (2013).

[28] F. Gutsch, Markov-Ketten ohne detailliertes Gleichgewicht, Bachelor's thesis, Humboldt-Universität zu Berlin, 2014.

[29] J.-S. Wang, Clusters in the three-dimensional Ising model with a magnetic field, Physica A **161**, 249 (1989).

[30] P. G. Lauwers and V. Rittenberg, The critical 2D Ising model in a magnetic field. A Monte Carlo study using a Swendsen-Wang algorithm, Phys. Lett. B **233**, 197 (1989).

[31] M. Saito and M. Matsumoto, in *SIMD-oriented Fast Mersenne Twister: A 128-bit Pseudorandom Number Generator*, in *Monte Carlo and Quasi-Monte Carlo Methods 2006*, edited by A. Keller, S. Heinrich, and H. Niederreiter (Springer, Heidelberg, 2008); M. Saito, Master's thesis, Hiroshima University, 2007. The source code of the program is provided at http://www.math.sci.hiroshima-u.ac.jp/~m-mat/MT/SFMT/index.html.

[32] M. Hasenbusch, Thermodynamic Casimir effect: Universality and corrections to scaling, Phys. Rev. B **85**, 174421 (2012).

[33] M. Caselle and M. Hasenbusch, Universal amplitude ratios in the 3-D Ising model, J. Phys. A **30**, 4963 (1997).

[34] M. Campostrini, A. Pelissetto, P. Rossi, and E. Vicari, 25th-order high-temperature expansion results for three-dimensional Ising-like systems on the simple-cubic lattice, Phys. Rev. E **65**, 066127 (2002).